24th COBEM - 2017

24th ABCM International Congress of Mechanical Engineering
December 3-8, 2017, Curitiba, PR, Brazil

COBEM-2017-1463
A PRELIMINARY STUDY ON ACTIVE FLOW CONTROL APPLIED TO CROSSWIND STABILITY OF HIGH-SPEED TRAINS

Alexandre Felipe Medina
Federal University of Uberlandia, Av. Joao Naves de Avila, 2121, Uberlandia, Minas Gerais 38400-902, Brazil
alexandremedina@ufu.br

Francisco José de Souza
Federal University of Uberlandia, Av. Joao Naves de Avila, 2121, Uberlandia, Minas Gerais 38400-902, Brazil
francisco.souza@ufu.br

Carlos Antônio Ribeiro Duarte
Federal University of Uberlandia, Av. Joao Naves de Avila, 2121, Uberlandia, Minas Gerais 38400-902, Brazil
carlos.antonio.mec.ufu@gmail.com

Abstract. *Unsteady Reynolds-Averaged Navier-Stokes (URANS) simulation is used for analyzing the applicability of active control techniques on improving crosswind stability of trains. The analysis is made for an idealized* $1:25$ *scale high-speed train model for a Reynolds number of* $3.7 \cdot 10^5$*, based on the model height. The analysis is based on both momentum injection and suction techniques, the control velocity is set to* 1% *of the free-stream velocity. The analysis is made for different control locations where it is found that the control applied at the lee-side roof corner renders better results, reducing the lee-rail moment coefficient, mainly responsible for vehicle overturning in critical crosswind conditions.*

Keywords: *Crosswind Stability, Train Aerodynamics, URANS, Active Flow Control*

1. INTRODUCTION

In the last decades the world has witnessed a significant increase on the number of high-speed lines (HSL). In 2015 there was approximately 29,792 km of HSL in the world, with 3,602 high-speed train (HST) sets in operation in 20 countries (UIC , 2015). Not only the range and number of lines increased, the high-speed trains are faster. The first high-speed train in operation, the Japanese bullet train Shinkansen 0 Series, had a maximum operational speed of 200 km/h in 1964, while in 2015 the maximum speed in revenue operation was 350 km/h. The HSL are a transportation market which accommodates close to 1,600 million passenger per year (UIC , 2015). This expressive number of passenger combined with higher operating velocities achieved by modern trains has increased the concern of rail vehicles safety facing different issues during its operation, such as its stability under crosswind conditions.

The study of the stability of trains traveling in crosswind conditions dates back to the 1980's, mainly with experimental studies (Mair & Stewart , 1985; Baker , 1986; Copley , 1987; Chiu & Squire , 1992) and the start of numerical simulations (Chiu , 1995). With the development of image processing, as Particle Image Velocimetry (PIV), and new turbulence models, with Reynolds-averaged Navier-Stokes (RANS) (Diedrichs , 2008; Biadgo & Svorcan , 2014) and Large Eddy Simulation (LES) (Hemida & Krajnović , 2006; Waris et al. , 2007; Diedrichs , 2008) methods, more information could be obtained from wind-tunnel campaigns and simulations tests.

Recently, the study of active flow control applied to different problems in vehicle application has resurfaced, with the need to improve the aerodynamic efficiency of ground vehicles. The first studies were performed in the former National Advisory Committee for Aeronautics (NACA), a U.S. federal agency founded on March 3, 1915, to undertake, promote, and institutionalize aeronautical research. The first study on active flow control was presented in the work from Bamber (1931), where a complete study was performed on the use of flow injection to improve the aerodynamic efficiency of wings, by reducing the drag and increasing the generated lift, with similar studies found in the work from Kelly (1956); Han et al. (2013); Goodarzi et al. (2012). The latest studies found in the literature have focused on different active control techniques to suppress vortex structures behind bluff bodies (Muddada & Patnaik , 2010; Krajnović & Fernandes , 2011; Chaligné et al. , 2013; Han et al. , 2013; Barros et al. , 2016). This method is used to reduce the drag on vehicles, mainly applied to the automotive industry.

In this paper, unsteady RANS simulations (URANS) with two-equation turbulence models are made to analyze the applicability of active flow control techniques to improve crosswind stability of high-speed trains. The model used in this study is a generic idealized high-speed train under the influence of side winds at a yaw angle of $35°$. The Reynolds number is $3.7 \cdot 10^5$, based on the experimental results from Copley (1987) and Deliancourt (2015).

2. VALIDATION

In order to study the application of active flow control the idealized train proposed in the studies from Mair & Stewart (1985) and Copley (1987) is selected, as it is a simplification of a high-speed train geometry. This model is vastly study in different experimental wind-tunnel and numerical analysis (Hemida & Krajnović , 2006; Deliancourt , 2015), sources of results that are used to validate our numerical setup. The axis-symmetric 1:25 scale model has a height D of 126 mm and a slenderness ratio of 10, as shown in Figure 1. More information regarding the construction profile of the scale model can be found in the work from Copley (1987).

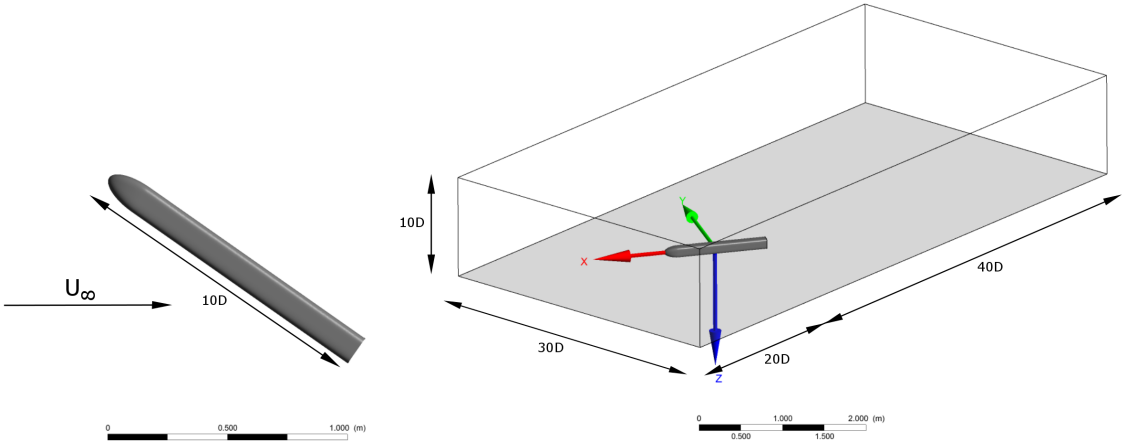

Figure 1. Simplified idealized model on 1:25 scale (left) and the computational domain with respective dimensions (right).

2.1 NUMERICAL SETUP

The numerical simulations were performed in the commercial solver ANSYS FLUENT, applying the URANS method. The Realizable $\kappa - \varepsilon$ (Shih et al. , 1995) and $\kappa - \omega$ SST (Menter , 1993) turbulence models were tested in the validation phase and compared with both experimental and numerical results. The computational domain characteristics are presented in Figure 1. Three different meshes were used in this study: two meshes with tetrahedral cells, with 1.5 and $2.5 \cdot 10^6$ elements, and one hexahedral cells mesh with $2.5 \cdot 10^6$ elements. The inlet is set as a block profile velocity-inlet. No-slip wall conditions are applied to the model and floor, with symmetry boundary conditions applied to the side and roof. The outlet is set as pressure-outlet with $0\ Pa$. The unsteady calculations are made with a time-step of $0.001\ s$ and a total simulation time of $1\ s$.

2.2 RESULTS

The validation results are compared with respect to the experimental data from Copley (1987) and Deliancourt (2015), and to the numerical results with LES model from Hemida & Krajnović (2006). The pressure distribution at X/D= 2.5 over a surface line around the train is presented in Figure 2, for an yaw angle of $\beta = 35°$. The overall analysis of the simulations show good agreement between the URANS calculations and both experimental results. Better performance is found for the SST turbulence models, where an overestimation is found for the pressure at $\theta = 90° - 180°$, which is the lee-side roof corner. This can be related to the boundary layer detachment and wake formation is this region. The best results were found for the SST turbulence model with the hexahedral mesh, which achieves better convergence and faster stabilization of the aerodynamic coefficients.

Comparing the simulation results from our SST model analysis and the experimental results for Copley (1987), one can observe the underestimation for the pressure distribution at $\theta = 225° - 315°$, which is the under-body region. This occurs since Copley (1987) tried to model the relative motion between train and ground, which was not modeled in our simulations, as our model is considered static. Compared to the experimental results from Deliancourt (2015), which also considered a static model, our analysis is fairly close, showing good agreement.

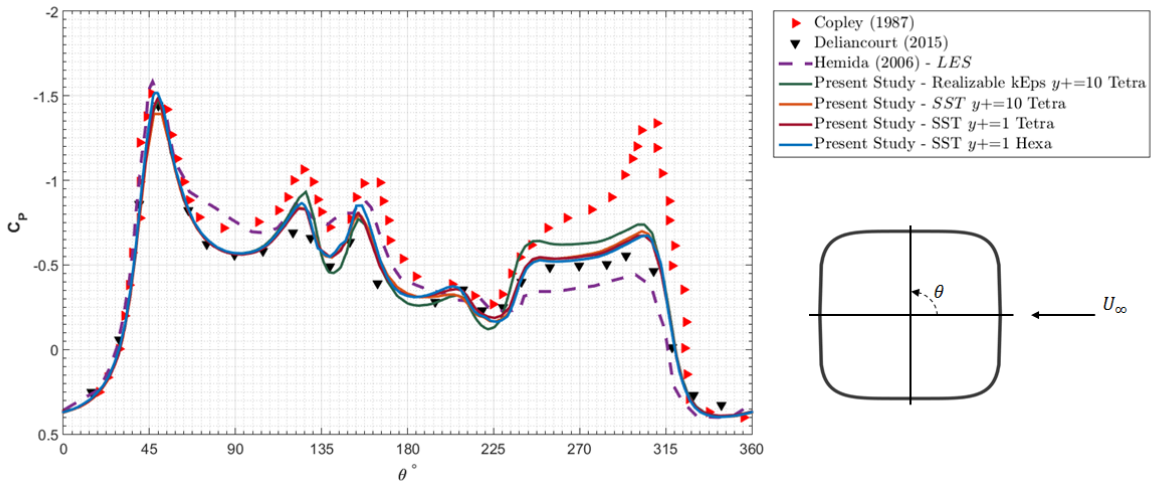

Figure 2. Pressure coefficient distribution over the train surface at X/D= 2.5 and $\beta = 35°$.

As the simulation setup considered in this analysis is closer to the experiments from Deliancourt (2015), the pressure distribution is also analyzed for an yaw angle of $\beta = 30°$, for two different locations: at X/D= 2.5 and X/D= 6.5, respectively close and far from the train nose. Close to the train nose we have good agreement between the simulation and the experimental data from Deliancourt (2015). The pressure distribution far from the train nose is overestimated by a large extent in the under-body region. However, it can be seen that even with this deviation from the experimental data, the qualitative form of the curve is similar for both cases.

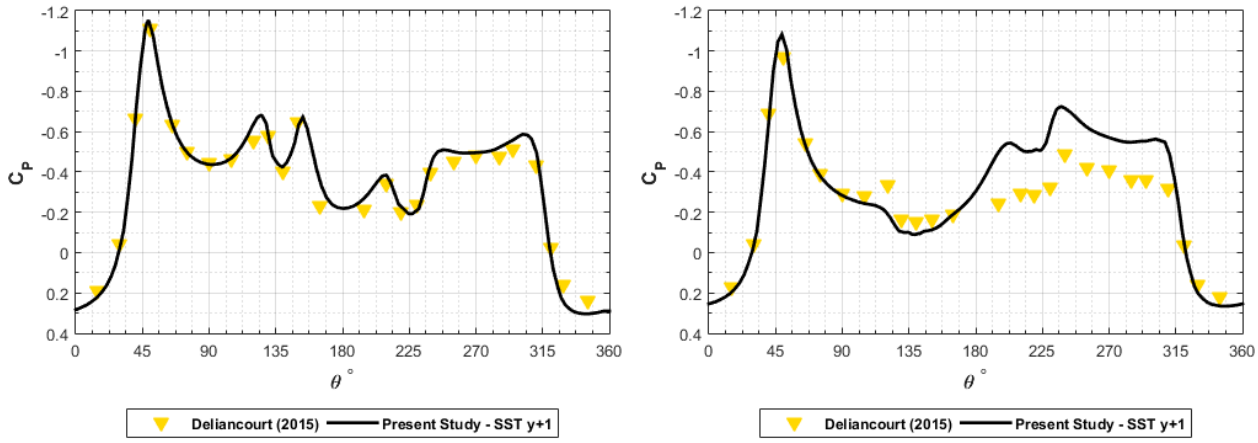

Figure 3. Pressure coefficient distribution over the train surface at X/D= 2.5 (left) and X/D= 6.5 (right), for $\beta = 30°$.

3. ACTIVE FLOW CONTROL ANALYSIS

The analysis of both injection and suction techniques are carried out in the finer mesh using the SST turbulence model, which presented the best agreement with respect to the experimental results. Three control regions were created, with three different lengths ($1D$, $2D$ and $3D$) and equal width for each position at the upper lee-side of the model (roof corned, Side 50% and Side 21% above the symmetry line), totaling eighteen control configurations (nine for the injection and nine for the suction technique). The control regions begin at $1.27D$ aft the nose, from where the cross-section presents a constant profile. The control velocity was set to be 1% of the free-stream velocity and the injection and suction directions are normal to the control surfaces, as shown in Figure 4.

The evaluation of improvement for the train crosswind stability relies on the aerodynamics coefficients. More precisely, it depends on the lee-rail moment coefficient, which is mainly responsible for overturning the train in critical conditions. This moment is calculated relative to the lee-rail, as exemplified in Figure 4. Hence, the active control improves the vehicle's stability if it achieves a lower moment coefficient over the lee-rail.

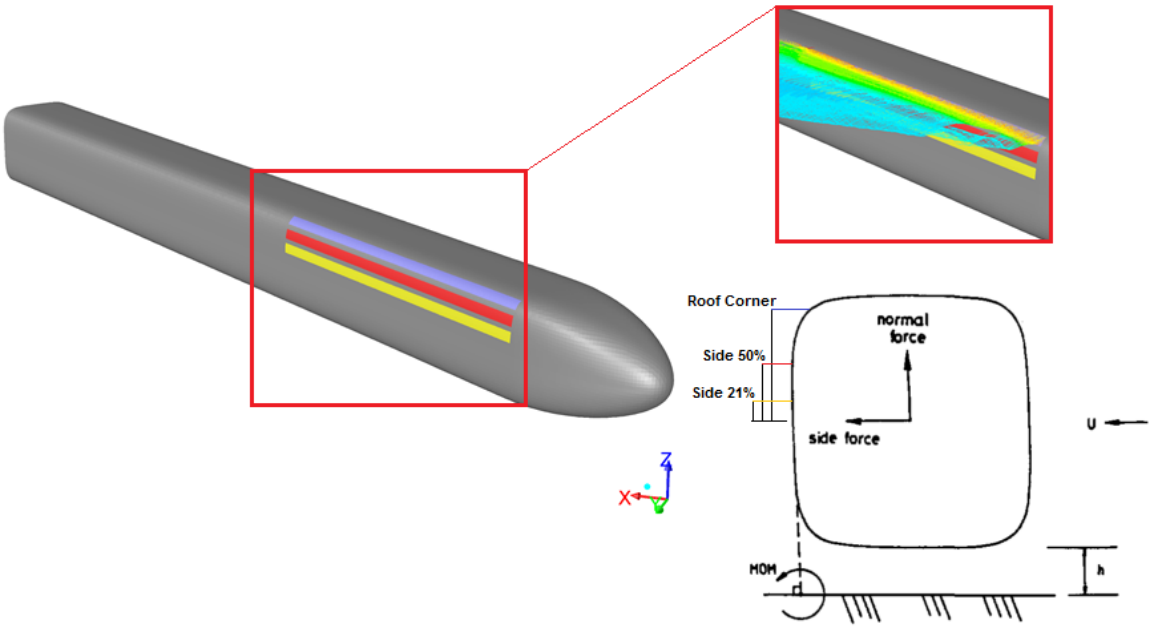

Figure 4. The location of the control regions at the lee-side roof corner (blue), 50% from the XY plane (red) and 21% from the XY plane (yellow); and the velocity colored streamlines from the roof corner injection control. And the Definition of the lee-rail moment, relative to the lee-rail (adapted from Copley Copley (1987)).

3.1 RESULTS

The results for the injection and suction techniques are presented in this section. First, we present a study of the best position for the control region by comparing the lee-rail moment coefficient for each case, at yaw angle $\beta = 35°$. In sequence we evaluate the performance of both injection and suction techniques for the best control position at different yaw angles.

3.1.1 EVALUATION OF THE CONTROL REGION POSITION

In this section we evaluate the decrease on the lee-rail moment coefficient for both injection and suction techniques at the three different location and for the three different control region's length, at an yaw angle of $\beta = 35°$. The analysis for the injection technique shows that the lee-rail moment coefficient is reduced as the length of the control region increases, which is expected as the mass flow increases with the length, since the injection velocity is maintained at 1% of the free-stream velocity for all the cases. The control at the lee-side roof corner is generally more effective than the other two locations for reduced lengths, whereas it achieve close to same moment reduction as the control regions at 50% side for a length of $3D$.

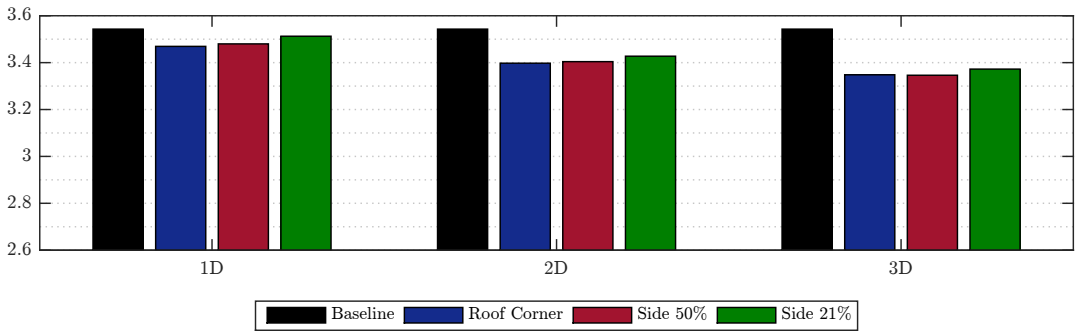

Figure 5. The lee-rail moment coefficient for different flow injection control locations and lengths, compared to the baseline idealized model.

The use of suction as means of control presented a less effective technique for control lengths of $1D$ and $2D$, as presented in Figure 6. This behavior was initially expected. For the injection technique the injected flow is expected to push the flow in the train vicinity, which reacts and produces a force in the train surface in the opposite direction of both control flow and free-stream flow. This effect is expected to be more effective than the suction technique. However, exceptionally for the suction technique applied to a control region with length of 3D at the lee-side roof corner, the reduction on the lee-rail rolling moment is higher than injecting flow. For both control techniques, greater reduction of the lee-rail moment coefficient was found for the longer control region, with length $3D$.

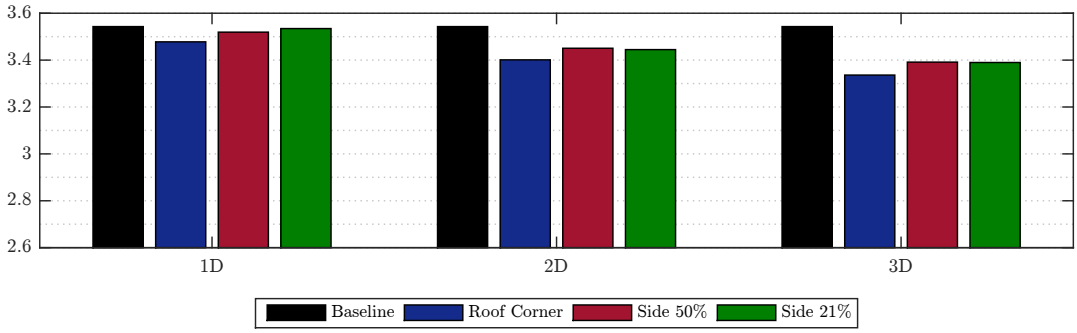

Figure 6. The lee-rail moment coefficient for different flow suction control locations and lengths, compared to the baseline idealized model.

A comparison between both techniques for a control region with length of $3D$ is presented Figure 7. For the analysis at $\beta = 35°$, setting the control velocity to 1% of the free-stream velocity, a maximum reduction of 5.8% of the lee-rail moment coefficient was found for a suction control at the lee-side roof corner, for a region with length of $3D$. For both studied techniques, the best location to apply an active flow control to improve the train's lateral stability under crosswind is the lee-side roof corner.

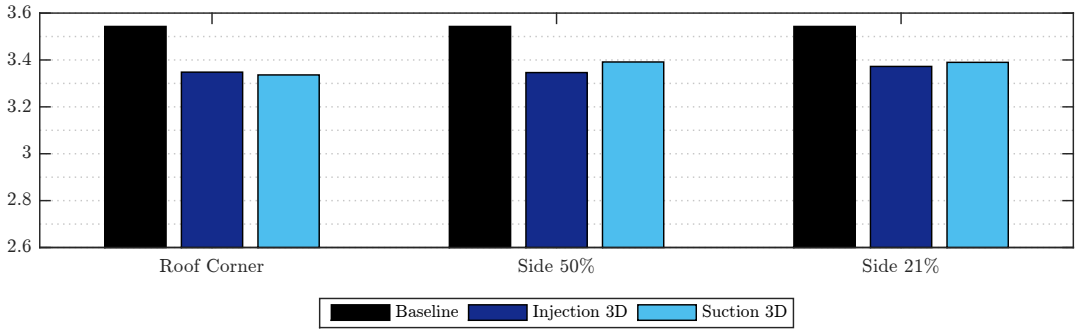

Figure 7. Comparison of the flow injection and suction techniques for different control locations with a control region with length of $3D$.

3.1.2 EVALUATION OF THE INJECTION CONTROL TECHNIQUES AT DIFFERENT YAW ANGLES

The comparison between the injection and suction techniques for different yaw angles at the best control location, the roof corner, is presented in this section. The risk of train derailment increases as the yaw angle increases, caused by the enlargement of the wake dimensions and its intensity. Figure 8 exemplifies this behavior as the lee-rail moment coefficient increases with the yaw angle. From Figure 8 it is possible to observe that both techniques present similar values of reduction on the lee-rail coefficient, which is better presented in Figure 9. At low yaw angles, both techniques present similar reduction, where the suction technique is slightly better. As the yaw angle increases the difference between both techniques is visible, where the suction technique perform approximately 0.5% better than injection, at an yaw angle of $\beta = 35°$, and approximately 2.5% better than injection, at an yaw angle of $\beta = 45°$.

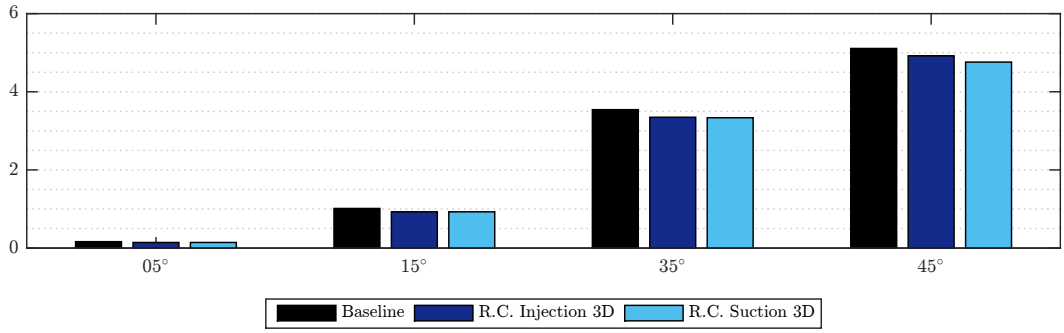

Figure 8. Comparison of the flow injection and suction techniques at the roof corner location, with a control region with length of $3D$, at different yaw angles.

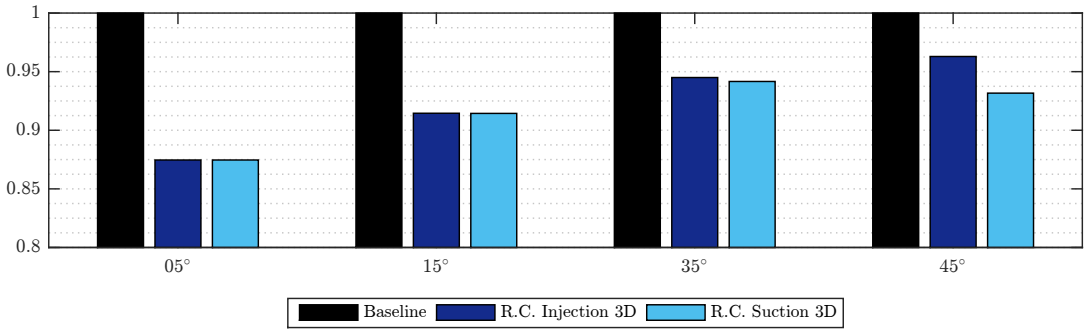

Figure 9. Comparison of the flow injection and suction techniques at the roof corner location, with a control region with length of $3D$, at different yaw angles.

4. CONCLUSIONS

The analysis of the use of URANS methodology on crosswind stability, although performed in a simplified idealized train, shows good agreement with experimental data. The preliminary results obtained for the active flow control applied to different yaw angles shows a good reduction on the lee-rail moment coefficient. As this moment coefficient is crucial to crosswind stability analysis, as is the one that could lead to trains overturning, the results shows that both injection and suction techniques can an option in order to control the train's stability when traveling under crosswind conditions.

5. ACKNOWLEDGEMENTS

The authors would like to thank the development agencies FAPEMIG, CNPq and CAPES, from the Brazilian government, and the computational support provided by the Fluid Mechanics Laboratory - MFLab, from the Faculty of Mechanical Engineering - FEMEC, Federal University of Uberlândia - UFU.

6. REFERENCES

International Union of Railways (UIC). High Speed Rail: Fast Track to Sustainable Mobility. 2015.

Mair, W. A.; Stewart, A. J. The flow past yawed slender bodies, with and without ground effects. *Journal of Wind Engineering and Industrial Aerodynamics*, v. 18, n. 3, p. 301–328, 1985. ISSN 01676105.

Baker, C. Train aerodynamic forces and moments from moving model experiments. *Journal of Wind Engineering and Industrial Aerodynamics*, v. 24, n. 3, p. 227–251, 1986. ISSN 01676105.

Copley, J. The Three-Dimensional Flow around Railway Trains. *Journal of Wind Engineering and Industrial Aerodynamics*, v. 26, p. 21–52, 1987.

Chiu, T.; Squire, L. An experimental study of the flow over a train in a crosswind at large yaw angles up to 90°. *Journal of Wind Engineering and Industrial Aerodynamics*, v. 45, p.47–74, 1992. ISSN 01676105.

Chiu, T. Prediction of the aerodynamic loads on a railway train in a cross-wind at large yaw angles using an integrated two- and three-dimensional source/vortex panel method. *Journal of Wind Engineering and Industrial Aerodynamics*, v. 57, p.19–39, 1995. ISSN 01676105.

Deliancourt, F. *Etude de l'aérodynamique des trains en situation de vents traversiers: impact de la présence d'appendices*. 184 p. Tese (Autre) — ISAE-ENSMA École Nationale Supérieure de Mécanique et D'Aérotechnique - Poitiers, 2015.

Diedrichs, B. Aerodynamic calculations of crosswind stability of a high-speed train using control volumes of arbitrary polyhedral shape. In: *BBAA VI International Colloquium on: Bluff Bodies Aerodynamics & Applications*. Milano, Italy: [s.n.], 2008. p. 20–24.

Biadgo, A. M.; Svorcan, J. Numerical investigation on the aerodynamics characteristics of high-speed train under turbulent crosswind. *Journal of Modern Transportation*, p.1–10, 2014. DOI 10.1007/s40534-014-0058-7.

Hemida, H.; Krajnović, S. Exploring the flow around a generic high-speed train under the influence of side winds using LES. In: *The Fourth International Symposium on Computational Wind Engineering*. Yokohama, Japan: [s.n.], 2006. p. 1–6.

Waris, M. B.; Ishihara, T.; Sarwar, M. W.; Fujino, Y. Numerical study of aerodynamic forces on trains in crosswind using LES turbulence model. In: *12th International Conference on Wind Engineering*. Cairns, Australia: [s.n.], 2007. p. 551–558.

Bamber, M. J. Wind Tunnel Tests on Airfoil Boundary Layer Control using a Backward Opening Slot. *National Advisory Committee for Aeronautics*, Report no. 385, 1931.

Kelly, M. W. Analysis of some parameters used in correlating Blowing-Type Boundary-Layer Control Data. *National Advisory Committee for Aeronautics*, Research Memorandum RM A56F12, 1956.

Huang, L. *Optimization of Blowing and Suction Control on NACA 0012 Airfoil using Genetic Algorithm with Diversity Control*. 113 p. Thesis (Ph.D.) — University of Kentucky Doctoral Dissertations, Kentucky, USA, 2004.

Goodarzi, M.; Rahimi, M.; Fereidouni, R. Investigation of Active Flow Control over NACA 0015 Airfoil Via Blowing. *International Journal of Aerospace Sciences*, v. 1, n. 4, p. 57–63, 2012.

Muddada, S.; Patnaik, B. An active flow control strategy for the suppression of vortex structures behind a circular cylinder. *European Journal of Mechanics/B Fluids*, v. 29, n. 2, p. 93–104, 2010. ISSN 0997-7546.

Krajnović, S.; Fernandes, J. Numerical simulation of the flow around a simplified vehicle model with active flow control. *International Journal of Heat and Fluid Flow*, v. 32, n. 1, p. 192–200, 2011. ISSN 0142727X.

Chaligné, S.; Castelain, T.; Michard, M. et al. Active control of the flow behind a two-dimensional bluff body in ground proximity. *Comptes Rendus MÃl'canique*, v. 341, n. 3, p. 289–297, 2013. ISSN 16310721.

Han, X.; Krajnović, S.; Basara, B. Study of active flow control for a simplified vehicle model using the PANS method. *International Journal of Heat and Fluid Flow*, v. 42, p. 139–150, 2013. ISSN 0142727X.

Barros, B.; Boree, J.; Noack, B. et al. Bluff body drag manipulation using pulsed jets and Coanda effect. *Journal of Fluid Mechanics*, v. 805, p. 422–459, 2016. ISSN 0022-1120.

Shih, T. H.; Liou, W. W.; Shabbir, A. et al. A new $\kappa - \varepsilon$ eddy viscosity model for high reynolds number turbulent flows. *Computers & Fluids*, v. 24, n. 3, p. 227–238, 1995. ISSN 00457930.

Menter, F. R. Zonal Two Equation $\kappa - \omega$ Turbulence Models for Aerodynamic Flows. In: *24th AIAA Fluid Dynamics Conference*. Orlando, FL: AIAA, 1993. p. 22.

7. RESPONSIBILITY NOTICE

The authors are the only responsible for the printed material included in this paper.